Article

Surface Patterning with Two-Dimensional Porphyrin Supramolecular Arrays

Joe Otsuki, Emi Nagamine, Tomohide Kondo, Kosyo Iwasaki, Masumi Asakawa, and Koji Miyake

J. Am. Chem. Soc., **2005**, 127 (29), 10400-10405• DOI: 10.1021/ja0531778 • Publication Date (Web): 30 June 2005

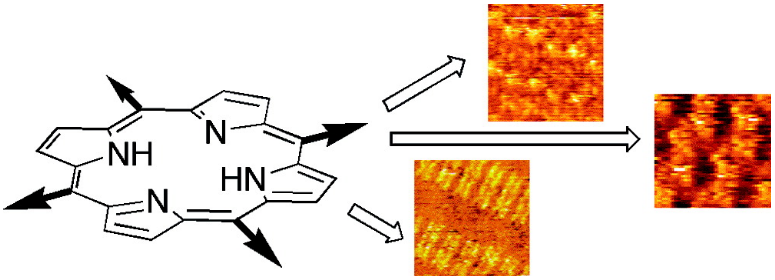

Journal of the American Chemical Society is published by the American Chemical Society. 1155 Sixteenth Street N.W., Washington, DC 20036

J|A|C|S
ARTICLES

Surface Patterning with Two-Dimensional Porphyrin Supramolecular Arrays

Joe Otsuki,*,† Emi Nagamine,† Tomohide Kondo,† Kosyo Iwasaki,†
Masumi Asakawa,‡ and Koji Miyake§

Contribution from the College of Science and Technology, Nihon University, 1-8-14 Kanda Surugadai, Chiyoda-ku, Tokyo 101-8308, Japan, Nanoarchitectonics Research Center (NARC), National Institute of Advanced Industrial Science and Technology (AIST), Tsukuba Central 5, 1-1-1 Higashi, Tsukuba, Ibaraki 305-8565, Japan, and Advanced Manufacturing Research Institute (AMRI), AIST, 1-2-1 Namiki, Tsukuba, Ibaraki 305-8564, Japan

Received May 16, 2005; E-mail: otsuki@chem.cst.nihon-u.ac.jp

Abstract: Monolayer arrays of a series of meso-tetra-substituted porphyrins containing octadecyloxy and carboxyl (or pyridyl) groups were prepared on the highly oriented pyrolytic graphite surface at the liquid/solid interface. It was found by means of scanning tunneling microscopy that some porphyrins from this family assemble into various patterns. Specifically, slightly undulated rows are obtained from 5,10,15-tris-(4-octadecyloxyphenyl)-20-(4-pyridyl)porphyrin. Meanwhile, rows with more pronounced kinks result from 5-(4-carboxyphenyl)-10,15,20-tris(4-octadecyloxyphenyl)porphyrin. The occurrence of the kinks is dependent on the arrangement of surrounding porphyrin molecules and is determined by intricate interplay between directional hydrogen-bonding interactions and packing forces, including molecule−molecule and molecule−substrate interactions. A double-layer structure is obtained from 5,10-bis(4-carboxyphenyl)-15,20-bis(4-octadecyloxyphenyl)porphyrin, probably through cyclic hydrogen bond formation. This work proves the concept that programmed surface patterning is possible by using porphyrins incorporating directional intermolecular interaction sites.

Introduction

Supramolecular chemistry has produced a number of increasingly complex, but well-defined, molecule-based assemblies by exploiting programmed information embedded in molecules for higher organization.[1] The concept of programmed intermolecular noncovalent forces has been applied mostly in solution and in crystals. Constructing supramolecules on surfaces, on the other hand, is an important and challenging theme in view of connecting molecular assemblies to the macroscopic world for potential applications in the field of molecular devices. Scanning tunneling microscopy (STM) provides chemists a unique opportunity to observe individual molecules in real space, once the molecules are immobilized on a surface.[2−7] Thus, there is plenty of room[8,9] at the surface as well, with the powerful aid of STM.

Surface assemblies from porphyrins are of special interest for their ample electronic and photonic properties, to name a few. In recent years, various porphyrin assemblies have been investigated on the atomically flat surfaces of highly oriented pyrolytic graphite (HOPG)[10−19] and metals.[20−26] The approach using HOPG is especially attractive for the study of two-dimensional assemblies, in that the experiments can be done under ambient conditions, and hence are less costly, and are amenable to all kinds of molecules if only soluble.[2−4] The assembly can be subjected to STM observations both at a liquid/solid interface and at an air/solid interface. Porphyrins applied on HOPG so far include alkylated derivatives[10−14] and elaborate multiporphyrin compounds,[15,16] among others.[17−19] Introducing long alkyl chains into a molecule is a versatile approach to

---

[†] Nihon University.

[‡] NARC, AIST.

[§] AMRI, AIST.

(1) Lehn, J.-M. *Supramolecular Chemistry: Concept and Perspectives*; VCH: Weinheim, 1995.

(2) Cyr, D. M.; Venkataraman, B.; Flynn, G. W. *Chem. Mater.* **1996**, *8*, 1600−1615.

(3) (a) De Feyter, S.; Hofkens, J.; Van der Auweraer, M.; Nolte, R. J. M.; Müllen, K.; De Schryver, F. C. *Chem. Commun.* **2001**, 585−592. (b) De Feyter, S.; De Schryver, F. C. *Chem. Soc. Rev.* **2003**, *32*, 139−150. (c) De Feyter, S.; De Schryver, F. C. *J. Phys. Chem. B* **2005**, *109*, 4290−4302.

(4) Samorí, P.; Rabe, J. P. *J. Phys. Condens. Matter.* **2002**, *14*, 9955−9973.

(5) Barth, J. V.; Weckesser, J.; Lin, N.; Dmitriev, A.; Kern, K. *Appl. Phys. A* **2003**, *76*, 645−652.

(6) Hecht, S. *Angew. Chem., Int. Ed.* **2003**, *42*, 24−26.

(7) Ruben, M. *Angew. Chem., Int. Ed.* **2005**, *44*, 1594−1596.

(8) Feynman, R. Presented at the Annual Meeting of the American Physical Society, Caltech, 1959; http://www.its.caltech.edu/~feynman/

(9) Lehn, J.-M. *Science* **1993**, *260*, 1762−1763.

(10) Ikeda, T.; Asakawa, M.; Goto, M.; Miyake, K.; Ishida, T.; Shimizu, T. *Langmuir* **2004**, *20*, 5454−5459.

(11) Ikeda, T.; Asakawa, M.; Miyake, K.; Shimizu, T. *Chem. Lett.* **2004**, *33*, 1418−1419.

(12) (a) Wang, H.; Wang, C.; Zeng, Q.; Xu, S.; Yin, S.; Xu, B.; Bai, C. *Surf. Interface Anal.* **2001**, *32*, 266−270. (b) Qiu, X.; Wang, C.; Zeng, Q.; Xu, B.; Yin, S.; Wang, H.; Xu, S.; Bai, C. *J. Am. Chem. Soc.* **2000**, *122*, 5550−5556. (c) Lei, S. B.; Wang, J.; Dong, Y. H.; Wang, C.; Wan, L. J.; Bai, C. L. *Surf. Interface Anal.* **2002**, *34*, 767−771.

(13) Zhou, Y.; Wang, B.; Zhu, M.; Hou, J. G. *Chem. Phys. Lett.* **2005**, *403*, 140−145.

(14) Ohshiro, T.; Ito, T.; Bühlmann, P.; Umezawa, Y. *Anal. Chem.* **2001**, *73*, 878−883.

(15) (a) Yin, J.; Guo, Q.; Palmer, R. E.; Bampos, N.; Sanders, J. K. M. *J. Phys. Chem. B* **2003**, *107*, 209−216. (b) Guo, Q.; Yin, J.; Yin, F.; Palmer, R. E.; Bampos, N.; Sanders, J. K. M. *J. Phys.: Condens. Matter* **2003**, *15*, S3127−S3138.

10.1021/ja0531778 CCC: $30.25 © 2005 American Chemical Society

Chart 1. Porphyrin Building Blocks for Two-Dimensional Arrays

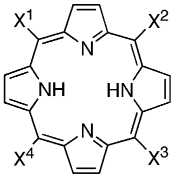

	X^1	X^2	X^3	X^4
C_4	$PhCO_2H$	$PhCO_2H$	$PhCO_2H$	$PhCO_2H$
C_3R_1	$PhCO_2H$	$PhCO_2H$	$PhCO_2H$	PhOR
***c*-C_2R_2**	$PhCO_2H$	$PhCO_2H$	PhOR	PhOR
***t*-C_2R_2**	$PhCO_2H$	PhOR	$PhCO_2H$	PhOR
C_1R_3	$PhCO_2H$	PhOR	PhOR	PhOR
R_4	PhOR	PhOR	PhOR	PhOR
P_4	Py	Py	Py	Py
P_3R_1	Py	Py	Py	PhOR
***c*-P_2R_2**	Py	Py	PhOR	PhOR
***t*-P_2R_2**	Py	PhOR	Py	PhOR
P_1R_3	Py	PhOR	PhOR	PhOR

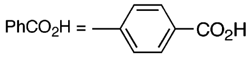

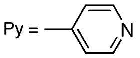

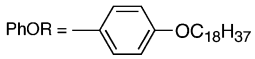

immobilize the alkylated molecule, due to the tendency of alkyl moieties to form closely packed arrays on HOPG.[2] Thus, 5,10,15,20-tetrakis(alkoxyphenyl)porphyrin (e.g. **R_4**, see Chart 1) forms a linear lamellar array, the alkyl chains from neighboring rows being interdigitated.[10−12]

Porphyrins may also be suitable as models in examining the relationship between the molecular structures and the supramolecular structures, since diverse substituents for intermolecular interactions can be synthetically introduced to the porphyrin scaffold in different symmetries in a systematic way. We reasoned that introducing directional forces such as hydrogen bonding, especially in less than 4-fold symmetrical ways, might produce novel patterns on surfaces. Hydrogen bonding has been used in non-porphyrinoid compounds and found to have a great impact on the surface assembly structures.[3,5]

There is some precedent for surface assemblies of porphyrins with hydrogen-bonding capability. The porphyrin with four carboxyl moieties in a 4-fold symmetry, 5,10,15,20-tetrakis(4-carboxyphenyl)porphyrin (**C_4**), when coadsorbed with stearic acid, forms a hydrogen-bonded network, resulting in an arrangement in a 4-fold symmetry on HOPG.[17] Another porphyrin derivative with one hydroxyl group, 5-(4-hydroxyphenyl)-10,15,20-tris(4-dedecyloxyphenyl)porphyrinatozinc(II), adsorbs on HOPG, adopting a face-on or an edge-on style, the involvement of the hydroxyl groups in hydrogen bonding being implied in both of the assemblies.[13] Systematic investigation into the effect of the positions and numbers of carboxyl groups on the porphyrin core on the supramolecular structures has only been done on the Au(111) surface under ultra-high-vacuum environments at a low temperature of 63 K, using carboxyphenyl- and 3,5-di-*tert*-butylphenyl-substituted porphyrins.[20]

We have investigated surface assemblies at the liquid/solid interface on HOPG from *meso*-tetrasubstituted porphyrins having both octadecyloxyphenyl and carboxyphenyl groups in all possible configurations. Also included in the study are porphyrins with octadecyloxyphenyl and pyridyl groups in all possible combinations (see Chart 1). We have obtained new two-dimensional patterns from three of the less symmetrical porphyrins, i.e., **P_1R_3**, **C_1R_3**, and ***c*-C_2R_2**, proving the concept that programmed surface patterning is possible by using porphyrins incorporating directional intermolecular interaction sites, as we describe herein.

Experimental Procedures

Synthesis. Reactions were carried out in the dark by wrapping the flask with aluminum foil to protect it from ambient light. Column chromatography was performed using Kanto Chemical silica gel (SiO_2) 60N. Recycle GPC was conducted using $CHCl_3$ as eluent on a Japan Analytical Industry LC-9201 system equipped with Jaigel-2H and Jaigel-1H columns in tandem, with exclusion limits of 5000 and 1000, respectively. ^1H NMR spectra were recorded on a JEOL GX400 spectrometer. High-resolution mass spectra (HRMS) of sample solutions in $CHCl_3$ were taken on an Agilent G1969A system with an atmospheric pressure chemical ionization (CI) chamber and a time-of-flight mass spectrometer. The purity of the prepared samples was carefully confirmed with TLC, GPC, and ^1H NMR data.

Methyl Esters of Porphyrins Containing Carboxyphenyl and Octadecyloxyphenyl Groups. The reaction conditions were taken from a reported procedure.[27] Pyrrole (2.73 g, 40.8 mmol) was added dropwise to a mixture of methyl 4-formylbenzoate (1.74 g, 10.6 mmol), 4-octadecyloxybenzaldehyde (11.3 g, 30.2 mmol), and $Zn(OAc)_2{\cdot}H_2O$ (1.89 g, 9.58 mmol) in propionic acid (200 mL), and the solution was stirred at room temperature for 1 h and then refluxed for 4 h. The solvent was removed to yield a black solid, which was passed through a SiO_2 column. Fractions that emit red fluorescence were collected to afford a purple solid. This solid, together with pyridine (0.8 mL) and 2,3-dichloro-5,6-dicyanobenzoquinone (0.81 g, 3.6 mmol), was dissolved in CH_2Cl_2 (100 mL), which was refluxed for 1 h. This solution was washed with 18% hydrochloric acid (40 mL × 3), saturated aqueous $NaHCO_3$ (40 mL × 3), and then brine (40 mL). Drying on Na_2SO_4 and removal of solvent afforded an isomeric mixture of porphyrins. Repeated chromatography (SiO_2, $CHCl_3$ to CH_2Cl_2) afforded pure isomers.

Trimethyl Ester of C_3R_1. R_f (SiO_2, $CHCl_3$) = 0.14. ^1H NMR ($CDCl_3$): $\delta = -2.80$ (2H, s, NH), 0.87 (3H, t, $J = 7$ Hz, RCH_3), 1.2−1.5 (28H, m, CH_2), 1.63 (2H, quintet, $J = 7$ Hz, $OCCCH_2$), 1.99 (2H, quintet, $J = 7$ Hz, $OCCH_2$), 4.11 (9H, s, OCH_3), 4.25 (2H, t, $J = 7$ Hz, OCH_2), 7.28 (2H, d, $J = 8$ Hz, ROPhH), 8.10 (2H, d, $J = 8$ Hz, ROPhH), 8.30 (6H, d, $J = 8$ Hz, CO_2PhH), 8.44 (6H, d, $J = 8$ Hz, CO_2PhH), 8.79 (2H, d, $J = 4$ Hz, β), 8.81 (4H, s, β), 8.92 (2H, d, $J = 4$ Hz, β). CI−HRMS: m/z calcd for $C_{68}H_{73}N_4O_7$ ($[M + H]^+$), 1057.5473; found, 1057.5440.

---

(16) Elemans, J. A. A. W.; Lensen, M. C.; Gerritsen, J. W.; van Kempen, H.; Speller, S.; Nolte, R. J. M.; Rowan, A. E. *Adv. Mater.* **2003**, *15*, 2070−2073.

(17) Lei, S. B.; Wang, C.; Yin, S. X.; Wang, H. N.; Xi, F.; Liu, H. W.; Xu, B.; Wan, L. J.; Bai, C. L. *J. Phys. Chem. B* **2001**, *105*, 10838−10841.

(18) Liu, Y.; Lei, S.; Yin, S.; Xu, S.; Zheng, Q.; Zeng, Q.; Wang, C.; Wan, L.; Bai, C. *J. Phys. Chem. B* **2002**, *106*, 12569−12574.

(19) Tao, N. J. *Phys. Rev. Lett.* **1996**, *76*, 4066−4069.

(20) Yokoyama, T.; Kamikado, T.; Yokoyama, S.; Mashiko, S. *J. Chem. Phys.* **2004**, *121*, 11993−11997.

(21) Yokoyama T.; Yokoyama, S.; Kamikado, T.; Okuno, Y.; Mashiko, S. *Nature* **2001**, *413*, 619−621.

(22) Yanagi, H.; Mukai, H.; Ikuta, K.; Shibutani, T.; Kamikado, T.; Yokoyama, S.; Mashiko, S. *Nano Lett.* **2002**, *2*, 601−604.

(23) Qiu, X.; Nazin, G. V.; Hotzel, A.; Ho, W. *J. Am. Chem. Soc.* **2002**, *124*, 14804−14809.

(24) (a) Hipps, K. W.; Scudiero, L.; Barlow, D. E.; Cooke, M. P., Jr. *J. Am. Chem. Soc.* **2002**, *124*, 2126−2127. (b) Scudiero, L.; Hipps, K. W.; Barlow, D. E. *J. Phys. Chem. B* **2003**, *107*, 2903−2909.

(25) (a) Suto, K.; Yoshimoto, S.; Itaya, K. *J. Am. Chem. Soc.* **2003**, *125*, 14976−14977. (b) Yoshimoto, S.; Tada, A.; Suto, K.; Narita, R.; Itaya, K. *Langmuir* **2003**, *19*, 672−677. (c) Yoshimoto, S.; Higa, N.; Itaya, K. *J. Am. Chem. Soc.* **2004**, *126*, 8540−8545. (d) Yoshimoto, S.; Inukai, J.; Tada, A.; Abe, T.; Morimoto, T.; Osuka, A.; Furuta, H.; Itaya, K. *J. Phys. Chem. B* **2004**, *108*, 1948−1954. (e) Yoshimoto, S.; Tada, A.; Suto, K.; Yau, S.-L.; Itaya, K. *Langmuir* **2004**, *20*, 3159−3165.

(26) He, Y.; Ye, T.; Borguet, E. *J. Am. Chem. Soc.* **2002**, *124*, 11964−11970.

(27) Matile, S.; Berova, N.; Nakanishi, K.; Fleischhauer, J.; Woody R. W. *J. Am. Chem. Soc.* **1996**, *118*, 5198−5206.

Dimethyl Ester of *c*-C_2R_2. R_f (SiO_2, $CHCl_3$) = 0.48. ^{1}H NMR ($CDCl_3$): $\delta = -2.77$ (2H, s, NH), 0.87 (6H, t, J = 7 Hz, RCH_3), 1.2−1.6 (56H, m, CH_2), 1.63 (4H, quintet, J = 7 Hz, $OCCCH_2$), 1.99 (4H, quintet, J = 7 Hz, $OCCH_2$), 4.11 (6H, s, OCH_3), 4.25 (4H, t, J = 7 Hz, OCH_2), 7.28 (4H, d, J = 8 Hz, ROPhH), 8.10 (4H, d, J = 8 Hz, ROPhH), 8.30 (4H, d, J = 8 Hz, CO_2PhH), 8.44 (4H, d, J = 8 Hz, CO_2PhH), 8.77 (2H, d, J = 5 Hz, β), 8.79 (2H, s, β), 8.89 (2H, s, β), 8.91 (2H, d, J = 5 Hz, β). CI−HRMS: m/z calcd for $C_{84}H_{107}N_4O_6$ ($[M + H]^+$), 1267.8185; found, 1267.8172.

Dimethyl Ester of *t*-C_2R_2. R_f (SiO_2, $CHCl_3$) = 0.60. ^{1}H NMR ($CDCl_3$): $\delta = -2.78$ (2H, s, NH), 0.87 (6H, t, J = 8 Hz, RCH_3), 1.2−1.5 (56H, m, CH_2), 1.62 (4H, quintet, J = 7 Hz, $OCCCH_2$), 1.98 (4H, quintet, J = 7 Hz, $OCCH_2$), 4.11 (6H, s, OCH_3), 4.25 (4H, t, J = 7 Hz, OCH_2), 7.28 (4H, d, J = 8 Hz, ROPhH), 8.09 (4H, d, J = 8 Hz, ROPhH), 8.30 (4H, d, J = 8 Hz, CO_2PhH), 8.44 (4H, d, J = 8 Hz, CO_2PhH), 8.78 (4H, d, J = 5 Hz, β), 8.94 (4H, d, J = 5 Hz, β). CI−HRMS: m/z calcd for $C_{84}H_{107}N_4O_6$ ($[M + H]^+$), 1267.8185; found, 1267.8172.

Methyl Ester of C_1R_3. R_f (SiO_2, $CHCl_3$) = 0.77. ^{1}H NMR ($CDCl_3$): $\delta = -2.76$ (2H, s, NH), 0.88 (9H, t, J = 7 Hz, RCH_3), 1.2−1.5 (84H, m, CH_2), 1.63 (6H, quintet, J = 7 Hz, $OCCCH_2$), 1.99 (6H, quintet, J = 8 Hz, $OCCH_2$), 4.11 (6H, s, OCH_3), 4.25 (6H, t, J = 7 Hz, OCH_2), 7.28 (6H, d, J = 8 Hz, ROPhH), 8.10 (6H, d, J = 8 Hz, ROPhH), 8.30 (2H, d, J = 8 Hz, CO_2PhH), 8.43 (2H, d, J = 8 Hz, CO_2PhH), 8.76 (2H, d, J = 4 Hz, β), 8.88 (4H, s, β), 8.89 (2H, d, J = 4 Hz, β). CI−HRMS: m/z calcd for $C_{100}H_{141}N_4O_5$ ($[M + H]^+$), 1479.0929; found, 1479.0933.

Porphyrins Containing Carboxyphenyl and Octadecyloxyphenyl Groups: General Procedure. The hydrolysis followed a reported procedure.[28] The purified methyl ester was suspended in a mixture of 2-propanol and 2 M aqueous KOH, which was refluxed for 6 h. The reaction, after being allowed to cool to room temperature, was acidified with concentrated HCl to pH ∼3, and extracted with $CHCl_3$. The organic layer was washed with saturated aqueous $NaHCO_3$ and dried over Na_2SO_4, and the solvent was evaporated to afford a residue.

C_3R_1. The residue was reprecipitated from MeOH and H_2O. R_f (SiO_2, $CHCl_3$/MeOH (9/1)) = 0.10. ^{1}H NMR (DMSO-d_6): $\delta = -2.94$ (2H, s, NH), 0.78 (3H, t, J = 7 Hz, CH_3), 1.2−1.5 (28H, m, CH_2), 1.52 (2H, quintet, J = 7 Hz, $OCCCH_2$), 1.87 (2H, quintet, J = 7 Hz, $OCCH_2$), 4.35 (2H, t, J = 7 Hz, OCH_2), 7.34 (2H, d, J = 8 Hz, ROPhH), 8.09 (2H, d, J = 8 Hz, ROPhH), 8.33 (6H, d, J = 8 Hz, CO_2PhH), 3.38 (6H, d, J = 8 Hz, CO_2PhH), 8.8−8.9 (8H, m, β). CI−HRMS: m/z calcd for $C_{65}H_{67}N_4O_7$ ($[M + H]^+$), 1015.5004; found, 1015.4982.

***c*-C_2R_2.** The residue was chromatographed (SiO_2, $CHCl_3$/MeOH (9/1)) and then reprecipitated from $CHCl_3$ and MeOH. Yield: 45%. R_f (SiO_2, $CHCl_3$/MeOH (9/1)) = 0.32. ^{1}H NMR ($CDCl_3$): $\delta = -2.75$ (2H, s, NH), 0.88 (6H, t, J = 7 Hz, CH_3), 1.2−1.7 (60H, m, CH_2), 2.00 (4H, quintet, J = 7 Hz, $OCCH_2$), 4.26 (4H, t, J = 7 Hz, OCH_2), 7.30 (4H, d, J = 8 Hz, ROPhH), 8.12 (4H, d, J = 8 Hz, ROPhH), 8.35 (4H, d, J = 8 Hz, CO_2PhH), 8.51 (4H, d, J = 8 Hz, CO_2PhH), 8.80 (2H, s, β), 8.81 (2H, d, J = 5 Hz, β), 8.91 (2H, s, β), 8.93 (2H, d, J = 5 Hz, β). CI−HRMS: m/z calcd for $C_{82}H_{103}N_4O_5$ ($[M + H]^+$), 1239.7872; found, 1239.7876.

***t*-C_2R_2.** The residue exhibited too low a solubility in usual solvents to be purified and characterized properly.

C_1R_3. The residue was chromatographed (SiO_2, $CHCl_3$/MeOH (10/0 to 9/1)). Yield: 95%. R_f (SiO_2, $CHCl_3$/MeOH (9/1)) = 0.63. ^{1}H NMR ($CDCl_3$): $\delta = -2.76$ (2H, s, NH), 0.88 (9H, t, J = 7 Hz, CH_3), 1.2−1.7 (90H, m, CH_2), 1.99 (6H, quintet, J = 7 Hz, $OCCH_2$), 4.26 (6H, t, J = 7 Hz, OCH_2), 7.28 (6H, d, J = 8 Hz, ROPhH), 8.10 (6H, d, J = 8 Hz, ROPhH), 8.34 (2H, d, J = 8 Hz, CO_2PhH), 8.49 (2H, d, J = 8 Hz, CO_2PhH), 8.78 (2H, d, J = 5 Hz, β), 8.89 (4H, s, β), 8.90 (2H, d, J = 5 Hz, β). CI−HRMS: m/z calcd for $C_{99}H_{138}N_4O_5$ ($[M]^+$), 1465.0773; found, 1465.0777.

Porphyrins Containing Pyridyl and Octadecyloxyphenyl Groups. The reaction conditions were taken from a reported procedure.[29] A solution of 4-octadecyloxybenzaldehyde (6.18 g, 16.5 mmol) and 4-pyridinaldehyde (5.42 g, 50 mmol) in propionic acid (250 mL) was stirred at room temperature for 1 h and then heated to reflux. Once the solution was boiling, pyrrole (4.65 mL, 67 mmol) was added dropwise. The reaction was stirred at reflux for 1 h and then at room temperature for 20 h. The residue obtained upon evaporation of the solvent was partitioned between $CHCl_3$ and H_2O, and the organic layer was put aside. The aqueous layer, which was neutralized with $NaHCO_3$, was extracted with $CHCl_3$. The residue obtained from the combined organics, after being dried over Na_2SO_4, was chromatographed. Each isomer was isolated through repeated SiO_2 column chromatography ($CHCl_3$/MeOH) and recycle GPC. Final materials were reprecipitated from CH_2Cl_2 and MeOH, if necessary, to remove contaminants from SiO_2 or solvents.

P_3R_1. R_f (SiO_2, $CHCl_3$/MeOH (9/1)) = 0.54. ^{1}H NMR ($CDCl_3$): $\delta = -2.87$ (2H, s, NH), 0.87 (3H, t, J = 7 Hz, CH_3), 1.2−1.5 (28H, m, CH_2), 1.63 (2H, quintet, J = 7 Hz, $OCCCH_2$), 1.99 (2H, quintet, J = 7 Hz, $OCCH_2$), 4.26 (2H, t, J = 7 Hz, OCH_2), 7.30 (2H, d, J = 8 Hz, Ph), 8.10 (2H, d, J = 8 Hz, Ph), 8.16 (6H, dd, J = 4 Hz, 1.5 Hz, py), 8.82 (2H, d, J = 4 Hz, β), 8.85 (4H, s, β), 8.97 (2H, d, J = 4 Hz, β), 9.05 (6H, dd, J = 4 Hz, 1.5 Hz, py). CI−HRMS: m/z calcd for $C_{59}H_{64}N_7O_1$ ($[M + H]^+$), 886.5094; found, 886.5161.

***c*-P_2R_2.** R_f (SiO_2, $CHCl_3$/MeOH (9/1)) = 0.69. ^{1}H NMR ($CDCl_3$): $\delta = -2.82$ (2H, s, NH), 0.87 (6H, t, J = 7 Hz, CH_3), 1.2−1.5 (56H, m, CH_2), 1.63 (4H, quintet, J = 7 Hz, $OCCCH_2$), 1.99 (4H, quintet, J = 7 Hz, $OCCH_2$), 4.26 (4H, t, J = 7 Hz, OCH_2), 7.29 (4H, d, J = 8 Hz, Ph), 8.10 (4H, d, J = 8 Hz, Ph), 8.16 (4H, dd, J = 4 Hz, 1.5 Hz, py), 8.79 (2H, d, J = 5 Hz, β), 8.83 (2H, s, β), 8.91 (2H, s, β), 8.94 (2H, d, J = 5 Hz, β), 9.04 (4H, dd, J = 4 Hz, 1.5 Hz, py). CI−HRMS: m/z calcd for $C_{78}H_{101}N_6O_2$ ($[M + H]^+$), 1153.7980; found, 1153.7987.

***t*-P_2R_2.** R_f (SiO_2, $CHCl_3$/MeOH (9/1)) = 0.91. ^{1}H NMR ($CDCl_3$): $\delta = -2.83$ (2H, s, NH), 0.87 (6H, t, J = 7 Hz, CH_3), 1.2−1.5 (56H, m, CH_2), 1.63 (4H, quintet, J = 7 Hz, $OCCCH_2$), 1.99 (4H, quintet, J = 7 Hz, $OCCH_2$), 4.26 (4H, t, J = 7 Hz, OCH_2), 7.29 (4H, d, J = 8 Hz, Ph), 8.10 (4H, d, J = 8 Hz, Ph), 8.17 (4H, dd, J = 4 Hz, 1.5 Hz, py), 8.80 (4H, d, J = 5 Hz, β), 8.94 (4H, d, J = 5 Hz, β), 9.04 (4H, dd, J = 4 Hz, 1.5 Hz, py). CI−HRMS: m/z calcd for $C_{78}H_{101}N_6O_2$ ($[M + H]^+$), 1153.7980; found, 1153.7982.

P_1R_3. R_f (SiO_2, $CHCl_3$/MeOH (9/1)) = 0.97. ^{1}H NMR ($CDCl_3$): $\delta = -2.78$ (2H, s, NH), 0.88 (9H, t, J = 7 Hz, CH_3), 1.2−1.5 (84H, m, CH_2), 1.63 (6H, quintet, J = 7 Hz, $OCCCH_2$), 1.99 (6H, quintet, J = 7 Hz, $OCCH_2$), 4.25 (6H, t, J = 7 Hz, OCH_2), 7.28 (6H, d, J = 8 Hz, Ph), 8.10 (6H, d, J = 8 Hz, Ph), 8.16 (2H, dd, J = 4 Hz, 1.5 Hz, py), 8.77 (2H, d, J = 5 Hz, β), 8.89 (4H, s, β), 8.92 (2H, d, J = 5 Hz, β), 9.02 (2H, dd, J = 4 Hz, 1.5 Hz, py). CI−HRMS: m/z calcd for $C_{97}H_{138}N_5O_3$ ($[M + H]^+$), 1422.0827; found, 1422.0867.

STM Measurements. *o*-Dichlorobenzene was purchased from Kanto Chemical and distilled before use. STM measurements were carried out with an SII SPI3800N-SPA400 microscope under ambient conditions. STM tips were made mechanically with Pt/Ir (9:1) wire. STM-1 grade HOPG was purchased from GE Advanced Ceramics. The uppermost layers of HOPG were peeled off with adhesive tape immediately before use. After the freshly cleaved HOPG was observed to confirm the atomic resolution of the tip, a droplet of a porphyrin solution in *o*-dichlorobenzene was applied on the surface just below the tip using a syringe. Usually, images could be taken for up to ∼30 min before the solvent evaporated. The concentration values in the text refer to the initial concentrations. The bias voltage refers to the substrate voltage with respect to the tip. Estimated errors in unit cell parameters a and b are ±0.2 nm, and that in θ is ±3°.

---

(28) Luo, C.; Guldi, D. M.; Imahori, H.; Tamaki, K.; Sakata, Y. *J. Am. Chem. Soc.* **2000**, *122*, 6535−6551.

(29) Avlasevich, Y. S.; Chevtchouk, T. A.; Knyukshto, V. N.; Kulinkovich, O. G.; Solovyov, K. N. *J. Porphyrins Phthalocyanines* **2000**, *4*, 579−587.

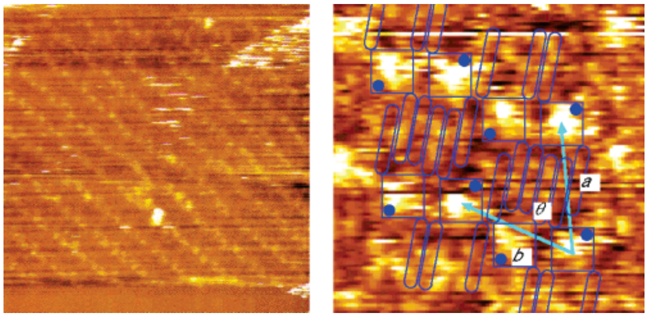

Figure 1. STM images for $\mathbf{P_1R_3}$ in *o*-dichlorobenzene (0.1 mM). (Left) 50 × 50 nm^2; tunneling conditions: $I = 98$ pA, $V = -0.80$ V. (Right) 10 × 10 nm^2; tunneling conditions: $I = 98$ pA, $V = -1.00$ V; $a = 4.2$ nm, $b = 3.9$ nm, $\theta = 69°$, Z (the number of molecules in a unit cell) = 2, A (the area of a unit cell) = 15.3 nm^2, $Z/A = 7.6$ nm^2. The blue dots indicate pyridyl groups.

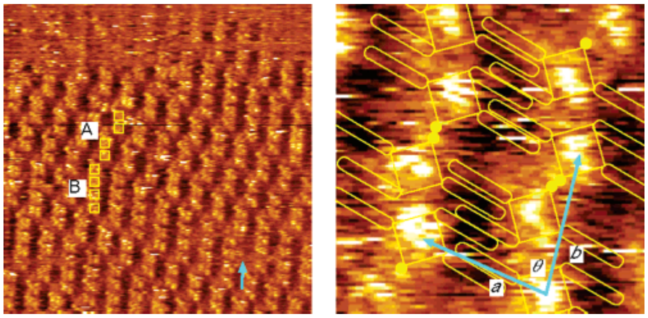

Figure 2. STM images for $\mathbf{C_1R_3}$ in *o*-dichlorobenzene (0.1 mM). (Left) 50 × 50 nm^2; tunneling conditions: $I = 49$ pA, $V = -1.15$ V. The arrow indicates a defect. (Right) 0.1 mM; 10 × 10 nm^2; tunneling conditions: $I = 20$ pA, $V = -1.20$ V; $a = 4.6$ nm, $b = 4.7$ nm, $\theta = 82°$, $Z = 2$, $A = 21.4$ nm^2, $Z/A = 10.7$ nm^2. Only pattern A (see text) is shown. The yellow dots indicate carboxyl groups.

Results

STM images for a 0.1 mM $\mathbf{P_1R_3}$ solution in *o*-dichlorobenzene on HOPG are shown in Figure 1. The images show rows similar to those of $\mathbf{R_4}$, but with a slight undulation in every other molecule. A schematic diagram of the most likely molecular arrangement is superimposed on the image in the right panel. The squares represent porphyrins, the sides being 13 Å in length, corresponding to the distance between the cis oxygen atoms in *meso*-tetrakis(4-methoxyphenyl)porphyrin, which is based on the crystal structure.[30,31] The rounded bars represent extended octadecyl chains, 22 Å long and 4.5 Å wide.[2] The dotted corners indicate pyridyl groups. In applying the structural model, it is assumed that alkyl chains adopt the fully extended conformation. The pyridyl group cannot participate in hydrogen bonding without a hydrogen-bond donor. Water molecules, present under ambient conditions, could participate in hydrogen bonding with the pyridyl groups. However, there is no evidence implying the involvement of the pyridyl groups in $\mathbf{P_1R_3}$ in hydrogen bonding in any form. The undulation may reduce the vacant space produced by the removal of alkyl chains from the array of $\mathbf{R_4}$.

The domain size of the array of $\mathbf{P_1R_3}$ is estimated to be much larger than 50 × 50 nm^2, since a domain boundary was rarely observed on repeated observation at different positions. We could obtain images for 0.5 and 1 mM samples, but the porphyrin images were more diffuse and the reproducibility was poor. A possible explanation is that more than one layer of porphyrins are deposited on the surface at the higher concentrations.

$\mathbf{C_1R_3}$ is similar to $\mathbf{P_1R_3}$ in terms of shape but with a carboxyl group that is capable of forming a complementary hydrogen bond. STM images for $\mathbf{C_1R_3}$ are shown in Figure 2. There are kinks every even number, i.e., 2 or 4, or rarely 6, of molecules on the row of molecules. A modeling on the image reveals that the carboxyl dimers form at these kinks. The porphyrin arrangement is shown by the schematics on the image in the right panel, and the carboxyl dimers are indicated with the pairs of dots. The center-to-center distance between the pair of $\mathbf{C_1R_3}$ molecules across the kink measures 2.5 nm. This is in agreement, within the experimental uncertainty, with the corresponding porphyrin−porphyrin separation in the crystal of 5,10,15,20-tetrakis(4-carboxyphenyl)porphyrinatozinc(II) (2.24 nm), in which the porphyrin units are connected with the hydrogen-bonded carboxyl dimers.[32] The close-packed structure has to be compromised by the hydrogen bond formation, since the carboxyl dimer formation would result in the appearance of void space on the surface; the surface occupancy per molecule increases from 7.6 nm^2 for $\mathbf{P_1R_3}$ to 10.7 nm^2 for $\mathbf{C_1R_3}$. The decrease in the surface density results in the reduction of interactions between alkyl chains as well as molecule−substrate interactions, as will be discussed later.

The competition is apparent from the observation that the kinks appear every other molecule in some places (pattern A), where hydrogen bonds dominate, whereas four or more molecules align linearly in other places (pattern B), where packing forces outweigh. In the rows of pattern B, there must be dangling carboxyl groups or at least carboxyl groups not participating in the optimal complementary hydrogen bond. There is communication between neighboring rows through alkyl−alkyl interactions; the number of molecules between kinks is the same as in the adjacent positions in the neighboring rows related by the *a* axis, in most of the cases. Interestingly, it was occasionally observed that patterns A and B coexist side by side, as indicated by the arrow in the left panel of Figure 2; pattern A is to the left and pattern B to the right of the arrow, resulting in a point defect. It is also the case that the size of a domain for the array of $\mathbf{C_1R_3}$ is much larger than 50 × 50 nm^2.

***c*-$\mathbf{C_2R_2}$** assembles into a double-layer structure, as shown in Figure 3. Each row consists of a pair of porphyrins in a head-to-head configuration. The same motif of interdigitation of alkyl chains as in the case of $\mathbf{R_4}$[10−12] fits nicely to the arrangement, as shown in the right panel. The cell parameters of the pseudo-unit-cell composed of the inner porphyrins (crossed in the right panel of Figure 3) across the alkyl layer (4.0 nm × 2.1 nm, 82°) are nearly identical with previously reported values for $\mathbf{R_4}$ (4.0 nm × 2.0 nm, 77°).[10] The value of *b* (2.1 nm) corresponds to the porphyrin−porphyrin separation along the row. The separation between the porphyrins making the head-to-head association across the row also measures 2.1 nm. This value is close to the porphyrin−porphyrin separation in $\mathbf{C_4}$ (1.9 nm), for which cyclic hydrogen bond formation is proposed, supported by molecular mechanics calculations.[17] Therefore, it is

---

(30) Hamor, M. J.; Hamor, T. A.; Hoard, J. L. *J. Am. Chem. Soc.* **1964**, *86*, 1938−1942.

(31) Mink, L. M.; Polam, J. R.; Christensen, K. A.; Bruck, M. A.; Walker, F. A. *J. Am. Chem. Soc.* **1995**, *117*, 9329−9339.

(32) Diskin-Posner, Y.; Goldberg, I. *Chem. Commun.* **1999**, 1961−1962.

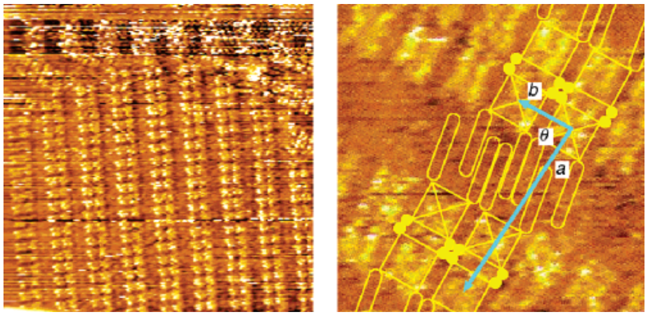

Figure 3. STM images for ***c*-C$_2$R$_2$** in *o*-dichlorobenzene (0.06 mM). (Left) 50 × 50 nm^2; tunneling conditions: $I = 63$ pA, $V = -1.10$ V. (Right) 10 × 10 nm^2; tunneling conditions: $I = 63$ pA, $V = -1.10$ V; $a = 5.8$ nm, $b = 2.1$ nm, $\theta = 82°$, $Z = 2$, $A = 12.1$ nm^2, $Z/A = 6.0$ nm^2. The yellow dots indicate carboxyl groups. Inner porphyrins are crossed, see the text.

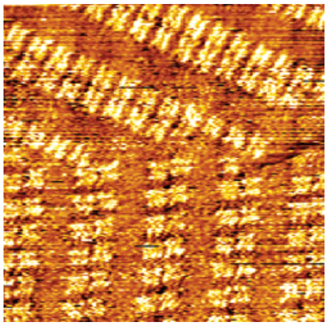

Figure 4. Domain boundary in the array of ***c*-C$_2$R$_2$** in *o*-dichlorobenzene (0.06 mM). 25 × 25 nm^2; tunneling conditions: $I = 63$ pA, $V = -1.10$ V.

likely that similar cyclic hydrogen bonds are formed in the spine of the rows, as represented by the associated four yellow dots in the right panel of Figure 3.

The domain sizes for the array of ***c*-C$_2$R$_2$** are not much larger than 50 × 50 nm^2, since we occasionally observed domain boundaries, such as the one shown in Figure 4. It would be anticipated that adjacent crystalline domains would orient at an angle of a multiple of 60°, as shown incidentally in the figure, if the underlying graphite surface determined the orientation of the molecular array.[2] However, there seems to be no definite correlation between the orientations of the adjacent crystalline domains, since we have sometimes encountered angles other than a multiple of 60° as well.

Discussion

To obtain STM images of molecules at the liquid/solid interface, some mutually conflicting requirements have to be met. First, an amount of molecules sufficient to cover the whole area must be adsorbed onto the surface from the solution, under the equilibrium between solution-phase molecules and adsorbed molecules. Hence, the concentration in the solution must be high enough. On the other hand, the concentration must be low to prevent undefined aggregate formation. In the case of porphyrins used in the present study, an aggregate may result through $\pi\pi$ stacking and hydrogen-bonding interactions at high concentrations. Also, there are some reports that show the concentration affects the morphology of surface assemblies not only at the molecular scale but at larger scale as well.[15,33] Hence, we have to find a concentration "window" in which a single layer of porphyrins forms on the surface. Incidentally, concentrations around 0.1 mM were found to be suitable for these porphyrins to give STM images under the present conditions, that is, at the *o*-dichlorobenzene/HOPG interface, in air, at room temperature, and under the atmospheric pressure. It should be noted, however, that the concentration is being changed under the microscope as the solvent evaporates.

Second, the adsorbed molecules must have a lateral mobility. Otherwise, scattered isolated molecules would be observed, since the molecules will not move from the position of first encounter with the surface. However, the molecules must be immobilized; that is, lateral diffusion must be frozen to give an STM image. This may be accomplished by forming a close-packed structure covering a large enough area. In practice, the class of porphyrin compounds in the present study have enough mobility, since we have never observed a clear image of isolated molecules in this and related[10,11] studies. Therefore, the key to obtain an STM image is the immobilization.

For the pyridyl derivatives studied in this study, we observed a surface pattern only of **P$_1$R$_3$**. It seems that at least three octadecyl chains are required to afford a stable adlayer for STM observation under the present conditions. The fact that a surface pattern is observed for ***c*-C$_2$R$_2$** but not for ***c*-P$_2$R$_2$** points to the importance of hydrogen bonding in stabilizing two-dimensional structures.

Close-packing of alkyl chains on HOPG is driven primarily by molecule−substrate interactions (adsorption energy) and secondarily by molecule−molecule interactions (two-dimensional crystallization energy). According to a molecular mechanics calculation by Bai et al.,[34] both of the energies are dominated by the van der Waals forces. The adsorption energies per CH$_2$ unit were estimated to be ca. −12 and −10 kJ mol^{-1} for the flat and vertical orientations of the alkyl chain, respectively, while the crystallization energies were estimated to be −5 and −6 kJ mol^{-1}, respectively. Another molecular mechanics calculation carried out by Rabe et al. indicated somewhat modest values of −7.7 to −8.0 kJ mol^{-1} for the adsorption potential per CH$_2$ unit, depending on the orientation of adsorbed alkane molecules.[35]

On the other hand, the binding energy in the optimal hydrogen-bonded dimer of carboxylic acid was estimated as −81 kJ mol^{-1}.[20] Let us estimate a gain or loss of energy on going from the closer-packed non-hydrogen-bonded **P$_1$R$_3$** to the looser-packed hydrogen-bonded **C$_1$R$_3$**. These porphyrins have three octadecyl chains, the adsorption energy amounting to −594 kJ mol^{-1}, using a value of −11 kJ mol^{-1} as the adsorption energy per CH$_2$ unit. The crystallization energies for both porphyrins are assumed to be the same, since bundles of six alkyl groups separated by void spaces are formed in both of them, as depicted in Figures 1 and 2. Thus, the energy loss associated with the looser packing for **C$_1$R$_3$** per unit area (1 nm^2) is 23 (= 594/7.6 − 594/10.7) kJ mol^{-1} nm^{-2}. If we use a value of −7.9 kJ mol^{-1} as the adsorption energy per CH$_2$ unit, the energy loss is 16 kJ mol^{-1}. Including the adsorption energy for the porphyrin core would further increase this energy loss. On the other hand, the

---

(33) Milic, T.; Garno, J. C.; Batteas, J. D.; Smeureanu, G.; Drain, C. M. *Langmuir* **2004**, *20*, 3974−3983.

(34) Yin, S.; Wang, C.; Qiu, X.; Xu, B.; Bai, C. *Surf. Interface Anal.* **2001**, *32*, 248−252.

(35) (a) Hentschke, R.; Schürmann, B. L.; Rabe, J. P. *J. Chem. Phys.* **1992**, *96*, 6213−6221. (b) Hentschke, R.; Schürmann, B. L.; Rabe, J. P. *J. Chem. Phys.* **1993**, *98*, 1756−1757.

gain in energy associated with the hydrogen bond formation per the unit area is 3.8 (= (81/10.7)/2) kJ mol^{-1} nm^{-2}. This estimation, albeit rough, shows that the former outweighs the latter by a large margin. Nevertheless, the STM observation showed that **C_1R_3** adopts the hydrogen-bond-directed void-rich, looser packing structure (pattern A), in competition with the alkyl-directed closer packing structure (pattern B), suggesting that these patterns are of comparable stability. This observation may point to the importance of the role of overlaying solvent in determining the assembly structure at the liquid/solid interface. The solvation by the solvent lowers the chemical potential of the solution-phase molecule, and thus helps the equilibrium shift to desorption, allowing less dense patterns. Also, the void space may be filled with the solvent molecules, although they may be highly mobile. Further, the contribution by the entropy term has to be taken into account for an exact depiction of the pattern formation.

The effect of alkyl chains on morphology is evident when comparing the results in the present work with the adlayers formed from porphyrins bearing 3,5-di-*tert*-butyl groups in place of octadecyloxy groups. Yokoyama et al. reported such structures of porphyrin assemblies on the surface of Au(111) at 63 K in ultra-high-vacuum STM.[20] Their analogue of **C_1R_3**, namely, 5-(4-carboxyphenyl)-10,15,20-tris(3,5-di-*tert*-butylphenyl)porphyrin, forms the optimal hydrogen-bonded dimer at low coverage, where double OH−O hydrogen bonds are involved. They observed that the integrity of the dimer is maintained even with increasing coverage. ***c*-C_2R_2** forms a double-row structure with a hydrogen-bonding network different from the optimal hydrogen-bonded dimers, while the aggregation of their analogue of ***c*-C_2R_2**, namely, 5,10-bis(4-carboxyphenyl)-15,20-bis-(3,5-di-*tert*-butylphenyl)porphyrin, involves the optimal hydrogen-bonded dimers to afford a tetramer at a low coverage. At higher coverages, the tetramers transform into a zigzag pattern due to a packing effect. However, the optimal hydrogen-bonded dimer structure is intact also in this case.

Conclusions and Prospects

In summary, we have demonstrated that specifically substituted porphyrins can produce a variety of surface patterns. The structure of the assembly is determined by an intricate interplay between directional hydrogen-bonding interactions and packing forces, including molecule−molecule and molecule−substrate interactions.

To understand fully the principles of surface supramolecular chemistry, further studies on many factors that influence the surface structure, including solvent, temperature, molecular structures, and so on, are needed. From a viewpoint of creating new structures, there is an immediate interest in what patterns will result from mixtures of carboxyl and pyridyl porphyrins. Beyond this, it is envisaged that diverse patterning may be possible by combining different, specifically programmed porphyrins.[36] Other interactions such as metal coordination[5,33,37] may also be utilized. Use of non-porphyrinoid molecules as structure-directing agents is another possibility. Finally, it may be possible to extend the assemblies in the direction normal to the surface by the use of axial coordination to surface-bound metalloporphyrins.[10,38] These projects aiming at controlling surface assemblies are underway in our laboratories.

Acknowledgment. This paper is dedicated to the 40th anniversary of Jean-Marie Lehn's Laboratory. This work was supported by funding from the Japan Ministry of Education, Science, Technology, Culture and Sports, Tokyo Ohka Foundation for the Promotion of Science and Technology, Saneyoshi Scholarship Foundation, and Nihon University.

JA0531778

---

(36) For three-dimensional crystal engineering of porphyrin, see: Goldberg, I. *Chem. Commun.* **2005**, 1243−1254.

(37) (a) Drain, C. M.; Nifiatis, F.; Vasenko, A.; Batteas, J. D. *Angew. Chem., Int. Ed.* **1998**, *37*, 2344−2347. (b) Drain, C. M.; Batteas, J. D.; Flynn, G. W.; Milic, T.; Chi, N.; Yablon, D. G.; Sommers, H. *Proc. Natl. Acad. Sci. U.S.A.* **2002**, *99*, 6498−6502. (c) Milic, T. N.; Chi, N.; Yablon, D. G.; Flynn, G. W.; Batteas, J. D.; Drain, C. M. *Angew. Chem., Int. Ed.* **2002**, *41*, 2117−2119.

(38) Otsuki, J. *Trends Phys. Chem.* **2001**, *8*, 61−72.